k_{t} Factorization for Hard Processes in Nuclei

Fabio Dominguez, Bo-Wen Xiao, and Feng Yuan

k_t-factorization for Hard Processes in Nuclei

Fabio Dominguez,[1] Bo-Wen Xiao,[2] and Feng Yuan[2,3]

[1]*Department of Physics, Columbia University, New York, NY, 10027*
[2]*Nuclear Science Division, Lawrence Berkeley National Laboratory, Berkeley, CA 94720*
[3]*RIKEN BNL Research Center, Building 510A,*
Brookhaven National Laboratory, Upton, NY 11973

Abstract

Two widely proposed k_t-dependent gluon distributions in the small-x saturation regime are investigated using two particle back-to-back correlations in high energy scattering processes. The Weizsäcker-Williams gluon distribution, interpreted as the number density of gluon inside nucleus, is studied in the quark-antiquark jet correlation in deep inelastic scattering. On the other hand, the unintegrated gluon distribution, defined as the Fourier transform of the color-dipole cross section, is probed in the direct photon-jet correlation in pA collisions. Dijet-correlation in pA collisions depends on both gluon distributions through combination and convolution in the large N_c limit.

As the foundation of high energy hadronic physics, QCD factorization enables us to separate the short distance perturbative physics from the long distance non-perturbative effects. Its prediction power relies on the universality of the parton distributions among different processes. Recent studies [1–7] have shown that the naive k_t-factorization is violated in two-particle production in hadron-hadron collisions. Nevertheless, in this letter, we establish an effective factorization in hard processes in nuclei scattered by a dilute probe by modifying the parton distributions at small-x. Although the parton distributions are no longer universal, they can be constructed from several universal individual building blocks.

The saturation phenomena in high energy hadronic interactions have attracted great attention in recent years. It has long been recognized that the gluon dynamics in QCD at small-x is responsible for these phenomena [8–11]. An effective theory, the color glass condensate (CGC), was proposed to systematically study this physics [11]. On the experimental side, there exist strong indications of the saturation from the structure function measurements in deep inelastic scattering (DIS) at HERA and the shadowing effects found in inclusive hadron production in dA collisions at RHIC [11]. Ongoing and future experiments from both RHIC and LHC, and in particular, the planned Electron-Ion Collider [12], shall provide further information on this.

An important aspect of the small-x gluon distribution function in nucleons and nuclei is the resummation of the multiple interactions of the hadronic probe with the target, because the gluon density is so high and these interactions have to be taken into account. In order to study the resummation effects, a transverse momentum dependence is introduced. They are referred to as the k_t-dependent gluon distributions, also called unintegrated gluon distribution (UGD) functions. Two different forms of the UGDs have been used in the literature. The first gluon distribution, also known as the Weizsäcker-Williams (WW) gluon distribution, measures the number density of gluons in the CGC formalism [10], whereas the second one defined as the Fourier transform of the color dipole cross section, appears in the calculations for, e.g., single inclusive particle production in pA collisions [11]. However, it has been argued that they can not be distinguished especially in the small $k_\perp$ region though they differ dramatically, and both of them are often used [13].

In this paper, we study two particle correlations in various high energy scattering processes as probes to these UGDs. There have been intensive investigations of these processes in the last few years [1–7]. Taking the quark distribution as an example, it was shown in Ref. [7] that, in the large nuclear number limit, an effective factorization can be achieved with modified parton distributions of nucleus in pA and γ^*A scattering processes where the multiple interaction effects can be resummed in the small-x formalism. Following this argument, we focus on the processes with a dilute system scattering on a dense target,

$$B + A \rightarrow H_1(k_1) + H_2(k_2) + X \ , \tag{1}$$

where A represents the dense target (such as a nucleus), B stands for the dilute projectile (such as nucleon or photon), H_1 and H_2 are the two final state particles with momenta k_1 and k_2, respectively. We are interested in the kinematic region where the transverse momentum imbalance between them is much smaller than the individual momentum: $q_\perp = |\vec{k}_{1\perp} + \vec{k}_{2\perp}| \ll P_\perp$ where $\vec{P}_\perp$ is defined as $(\vec{k}_{1\perp} - \vec{k}_{2\perp})/2$. This is referred as the back-to-back correlation limit (the correlation limit) in the following discussions. An important advantage of taking this limit is that we can apply the power counting method to obtain the leading order contribution of $q_\perp/P_\perp$ where the differential cross section directly depends on the UGDs of the nuclei. For example, the quark-antiquark jet correlation in deep inelastic

scattering (DIS) directly probes the first type of the UGD, whereas the direct photon-quark jet correlation in pA collisions probes the second type of UGD. The dijet (di-hadron) correlations in pA collisions can probe both gluon distributions, though the connection is more complicated.

Let us first discuss the conventional gluon distribution, generalized to include the transverse momentum dependence [14, 15],

$$xG^{(1)}(x, k_\perp) = \int \frac{d\xi^- d^2\xi_\perp}{(2\pi)^3 P^+} e^{ixP^+\xi^- - ik_\perp \cdot \xi_\perp}$$
$$\times \langle P|F^{+i}(\xi^-, \xi_\perp)\mathcal{L}_\xi^\dagger \mathcal{L}_0 F^{+i}(0)|P\rangle , \quad (2)$$

where $F^{\mu\nu}$ is the gauge field strength tensor $F_a^{\mu\nu} = \partial^\mu A_a^\nu - \partial^\nu A_a^\mu - g f_{abc} A_b^\mu A_c^\nu$ with f_{abc} the antisymmetric structure constants for $SU(3)$, and $\mathcal{L}_\xi = \mathcal{P} \exp\{-ig \int_{\xi^-}^\infty d\zeta^- A^+(\zeta, \xi_\perp)\}\mathcal{P} \exp\{-ig \int_{\xi_\perp}^\infty d\zeta_\perp \cdot A_\perp(\zeta^- = \infty, \zeta_\perp)\}$ is the gauge link in the adjoint representation $A^\mu = A_a^\mu t_a$ with $t_a = -if_{abc}$. It contains a transverse gauge link at spatial infinity which is important to make the definition gauge invariant [16]. These gauge links have to be made non-light-like to regulate the light-cone singularities when gluon radiation contributions are taken into account [14]. This does not affect the following analysis, because there is no light-cone singularity in the calculation. By choosing the light-cone gauge with certain boundary condition for the gauge potential (for example, in the above definition, $A_\perp(\zeta^- = \infty) = 0$), we can drop out the gauge link contribution, and find that this gluon distribution has the number density interpretation. Then, it can be calculated from the wave functions or the WW field of the nucleus target [10, 17]. At small-x for a large nucleus, it was found [10]

$$xG^{(1)}(x, k_\perp) = \frac{S_\perp}{\pi^2 \alpha_s} \frac{N_c^2 - 1}{N_c} \int \frac{d^2 r_\perp}{(2\pi)^2} \frac{e^{-ik_\perp \cdot r_\perp}}{r_\perp^2} \left(1 - e^{-\frac{r_\perp^2 Q_s^2}{4}}\right) , \quad (3)$$

where $N_c = 3$ is the number of colors and Q_s is the gluon saturation scale [11]. We have cross checked this result by directly calculating the gluon distribution function in Eq. (2) following the similar calculation for the quark in Ref. [16, 18].

Despite the nice physical interpretation, it has been argued that the gluon distribution in Eq. (2) is not directly related to physical observables in the CGC formalism. However, we will show that $xG^{(1)}$ can be directly probed through the quark-antiquark jet correlation in DIS,

$$\gamma_T^* A \to q(k_1) + \bar{q}(k_2) + X . \quad (4)$$

The calculations are performed for Q^2 in the same order of $P_\perp^2$ and the quarks are massless. Extension to the real photon scattering and/or massive quarks in the final state is straightforward. We will show the results for the transversely polarized photon, and that for the longitudinal one follows accordingly. We plot the typical Feynman diagram for the process of (4) in Fig. 1, where the bubble in the partonic part represents the hard interaction vertex including gluon attachments to both quark and antiquark lines. Fig. 1(a) is the leading Born diagram whose contributions can be associated with the hard partonic cross section times the gluon distribution from Eq. (2) [3]. In high energy scattering with the nucleus target, additional gluon attachments are important and we have to resum these contributions in the large nuclear number limit. Figs. 1(b,c) represent the diagrams contributing at two-gluon exchange order, where the second gluon can attach to either the quark line or the antiquark line. By applying the power counting method in the correlation limit ($q_\perp \ll P_\perp$), we can simplify the scattering amplitudes with the Eikonal approximation [3]. For example,
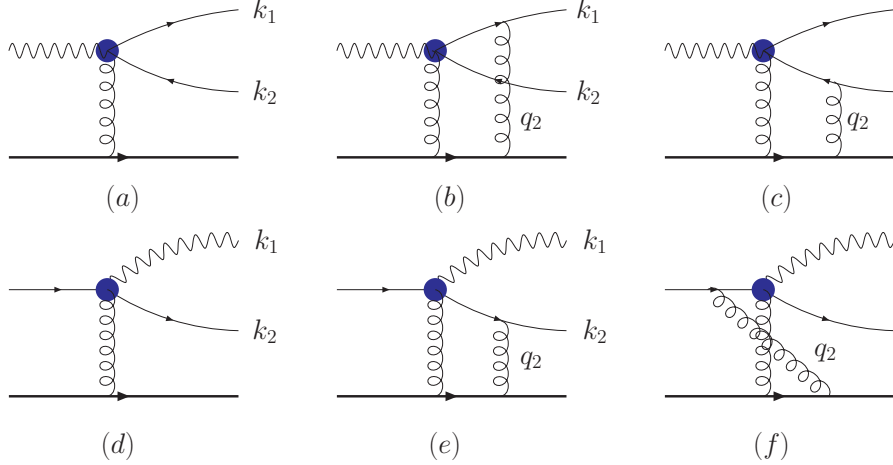
3

FIG. 1. Typical Feynman diagrams contributing to the quark-antiquark jet correlation in deep inelastic scattering (a,b,c) and photon-jet correlation in pA collisions (d,e,f): (a,d) leading order, where the bubble represents the gluon attachments to both quark lines; (b,c,e,f) two-gluon exchange diagrams.

Fig. 1(b) can be reduced to: $g/(-q_2^+ + i\epsilon)T^b\Gamma^a$ in the above limit, where q_2 is the gluon momentum, T^b is the $SU(3)$ color matrix in the fundamental representation and Γ^a represents the rest of the partonic scattering amplitude with color indices for the two gluons a and b. Similarly, Fig. 1(c) can be reduced to: $-g/(-q_2^+ + i\epsilon)\Gamma^aT^b$. The sum of these two diagrams will be $g/(-q_2^+ + i\epsilon)\left[T^b\Gamma^a - \Gamma^aT^b\right]$. Because of the unique color index in Γ_a, we find the effective vertex as,

$$\text{Fig. 1(b, c)} \sim \frac{i}{-q_2^+ + i\epsilon}(-ig)(-if_{bca})T^c \ , \tag{5}$$

which is exactly the first order expansion of the gauge link contribution in the gluon distribution defined in Eq. (2). Here, the crossing diagrams of Figs.1(b,c), by interchanging the two gluons, are included in the calculations to compare to the gauge link expansion results (see also Ref. [19]). For all high order contributions, we can follow the procedure outlined in Ref. [16] to derive the gluon distribution. Therefore, we obtain the following differential cross section for the quark-antiquark jet correlation in DIS process

$$\frac{d\sigma^{\gamma_T^* A \rightarrow q\bar{q}+X}}{d\mathcal{P}.\mathcal{S}.} = \delta(x_{\gamma^*} - 1)x_g G^{(1)}(x_g, q_\perp)H_{\gamma_T^*g \rightarrow q\bar{q}} \ , \tag{6}$$

where x_g is the momentum fraction carried by the gluon and is determined by the kinematics, $x_{\gamma^*} = z_q + z_{\bar{q}}$ with z_q and $z_{\bar{q}}$ being the momentum fractions of the virtual photon carried by the quark and antiquark, respectively. The phase space factor is defined as $d\mathcal{P}.\mathcal{S}. = dy_1 dy_2 d^2P_\perp d^2q_\perp$, and y_1 and y_2 are rapidities of the two outgoing particles. The leading order hard partonic cross section reads $H_{\gamma_T^*g \rightarrow q\bar{q}} = \alpha_s\alpha_{em}e_q^2(\hat{s}^2 + Q^4)/(\hat{s} + Q^2)^4 \times \left(\hat{u}/\hat{t} + \hat{t}/\hat{u}\right)$ with the usually defined partonic Mandelstam variables $\hat{s}$, $\hat{t}$ and $\hat{u}$. By taking $Q^2 = 0$, we can extend the above result to the case of dijet productions in real photons scattering on nuclei. The above process (4) can also be analyzed following the procedure in Ref. [2], where

4

the gluon distribution Eq. (2) is written in the fundamental representation,

$$xG^{(1)}(x, k_\perp) = 2 \int \frac{d\xi^- d\xi_\perp}{(2\pi)^3 P^+} e^{ixP^+\xi^- - ik_\perp \cdot \xi_\perp}$$

$$\times \langle P| \mathrm{Tr}\left[F^{+i}(\xi^-, \xi_\perp) \mathcal{U}^{[+]\dagger} F^{+i}(0) \mathcal{U}^{[+]} \right] |P\rangle , \qquad (7)$$

where the gauge link $\mathcal{U}_\xi^{[+]} = U^n[0, +\infty; 0]\, U^n[+\infty, \xi^-; \xi_\perp]$ with U^n being the light-like Wilson line in covariant gauge.

The quark-antiquark jet correlation in DIS (4) can also be calculated directly in the color-dipole and CGC formalism [20]. The basic element is the $q\bar{q}$ (color-dipole) wave function of the virtual photon, combined with the multi-scattering of the dipole on the nuclear target. Following this formalism, the amplitude can be written as

$$|\mathcal{A}|^2 = N_c \alpha_{em} e_q^2 \int \frac{\mathrm{d}^2 x}{(2\pi)^2} \frac{\mathrm{d}^2 x'}{(2\pi)^2} \frac{\mathrm{d}^2 b}{(2\pi)^2} \frac{\mathrm{d}^2 b'}{(2\pi)^2} e^{-ik_{1\perp} \cdot (x-x')}$$

$$\times e^{-ik_{2\perp} \cdot (b-b')} \sum \psi_T^*(x - b) \psi_T(x' - b')$$

$$\times \left[1 + S_{x_g}^{(4)}(x, b; b', x') - S_{x_g}^{(2)}(x, b) - S_{x_g}^{(2)}(b', x') \right] , \qquad (8)$$

where ψ_T is the $q\bar{q}$ Fock state wave function of a transversely polarized photon depending on $\epsilon_f^2 = z(1-z)Q^2$ with $z = z_q$, $S_{x_g}^{(2)}(x, b) = \frac{1}{N_c}\left\langle \mathrm{Tr}U(x)U^\dagger(b) \right\rangle_{x_g}$, $S_{x_g}^{(4)}(x, b; b', x') = \frac{1}{N_c}\left\langle \mathrm{Tr}U(x)U^\dagger(x')U(b')U^\dagger(b) \right\rangle_{x_g}$, and U is the Wilson line describing the multiple scatterings of a single quark with the nuclear target. The expectation value of multiple Wilson lines can be found in Refs. [20–22]. In order to study the differential cross section in the correlation limit, we substitute $u = x - b$ and $v = zx + (1-z)b$. Thus, the exponential factor becomes $e^{-iq_\perp \cdot (v-v')} e^{-i\tilde{P}_\perp \cdot (u-u')}$ where $\tilde{P}_\perp = (1-z)k_{1\perp} - zk_{2\perp} \approx P_\perp$. Then, we can expand the interaction part of the bracket at small u and u', but keep v and v' fixed. We find that the remaining contribution comes from the term involving inelastic scatterings while the elastic scattering part cancels out. Therefore, the square bracket in the above equation becomes $\frac{1}{N_c} u_i u_j' \left\langle \mathrm{Tr}\partial_i U(v)U^\dagger(v')\partial_j U(v')U^\dagger(v) \right\rangle_{x_g}$. With this expansion result, we further find that the wave function integral with $u_i u_j'$ leads to $\delta_{ij}(P_\perp^4 + \epsilon_f^4)/(P_\perp^2 + \epsilon_f^2)^2$, and the differential cross section can be simplified as,

$$\frac{d\sigma^{\gamma_T^* A \to q\bar{q}X}}{d\mathcal{P}.\mathcal{S}.} = \alpha_{em} e_q^2 \alpha_s \delta\left(x_{\gamma^*} - 1\right) z(1-z)\left(z^2 + (1-z)^2\right) \frac{P_\perp^4 + \epsilon_f^4}{(P_\perp^2 + \epsilon_f^2)^4}$$

$$\times (16\pi^3) \int \frac{d^3 v d^3 v'}{(2\pi)^6} e^{-iq_\perp \cdot (v-v')} 2 \left\langle \mathrm{Tr}F^{i+}(v)\mathcal{U}^{[+]\dagger} F^{i+}(v')\mathcal{U}^{[+]} \right\rangle_{x_g} . \qquad (9)$$

To compare with the differential cross section in Eq. (6), we notice that the partonic Mandelstam variables can be expressed in terms of $P_\perp$ and z as: $\hat{s} = P_\perp^2/(z(1-z))$, $\hat{t} = -(P_\perp^2 + \epsilon_f^2)/(1-z)$, and $\hat{u} = -(P_\perp^2 + \epsilon_f^2)/z$. Substituting these relations into Eq. (9), taking the small-x approximation for the gluon distribution, and correcting the normalization for the states in the calculation of the associated matrix elements, we find that it agrees with the factorization result (6) completely. This consistency is very important to demonstrate that we have a unified picture for the quark-antiquark correlation in DIS.

On the other hand, the direct photon-quark jet correlation in pA collisions,

$$pA \to \gamma(k_1) + q(k_2) + X , \qquad (10)$$

probes a different gluon distribution. We plot the relevant diagrams in Fig. 1 (d,e,f), again for the leading one gluon exchange and two gluon exchanges. Similarly, the two gluon exchange contributions can be summarized as

$$\text{Fig. 1(e, f)} \sim \frac{i}{-q_2^+ + i\epsilon}(-ig)\left(T^b\Gamma^a + \Gamma^a T^b\right) \; , \tag{11}$$

where the plus sign comes from the fact that the second gluon attaches to the quark line in the initial and final states. Since there is no color structure corresponding to Eq. (11), we can only express it in the fundamental representation. Following Ref. [2], we find that the gluon distribution in this process can be written as

$$xG^{(2)}(x, k_\perp) = 2 \int \frac{d\xi^- d\xi_\perp}{(2\pi)^3 P^+} e^{ixP^+\xi^- - ik_\perp \cdot \xi_\perp} \langle P|\text{Tr}\left[F^{+i}(\xi^-, \xi_\perp)\mathcal{U}^{[-]\dagger} F^{+i}(0)\mathcal{U}^{[+]}\right]|P\rangle \; , \tag{12}$$

where the gauge link $\mathcal{U}_\xi^{[-]} = U^n\left[0, -\infty; 0\right] U^n\left[-\infty, \xi^-; \xi_\perp\right]$. This gluon distribution can also be calculated in the CGC formalism where it is found to be $xG^{(2)}(x, q_\perp) \simeq \frac{q_\perp^2 N_c}{2\pi^2 \alpha_s} S_\perp F_{x_g}(q_\perp)$ with the normalized unintegrated gluon distribution $F_{x_g}(q_\perp) = \int \frac{d^2 r_\perp}{(2\pi)^2} e^{-iq_\perp \cdot r_\perp} S_{x_g}^{(2)}(0, r_\perp)$. Therefore, the differential cross section of (10) can be written as

$$\frac{d\sigma^{(pA \to \gamma q + X)}}{d\mathcal{P}.\mathcal{S}.} = \sum_f x_1 q(x_1) x_g G^{(2)}(x_g, q_\perp) H_{qg \to \gamma q} \; , \tag{13}$$

where $q(x_1)$ is the integrated quark distribution from the projectile nucleon. Because we are taking large nuclear number limit, the intrinsic transverse momentum associated with it can be neglected compared to that from the gluon distribution of nucleus. The hard partonic cross section is $H_{qg \to \gamma q} = \alpha_s \alpha_e e_q^2/(N_c \hat{s}^2)\left(-\hat{s}/\hat{u} - \hat{u}/\hat{s}\right)$. We can calculate process (10) in the CGC formalism directly [23], and again we find that these two calculations are consistent with each other.

The gluon distributions defined in Eqs. (2) and (12) have the same perturbative behavior and they reduce to the same gluon distribution after integrating over $k_\perp$. However, they do differ in the low transverse momentum region [11, 13]. It will be very important to measure the low $k_\perp$ behavior of the correlation processes of (4) and (10) to test these predictions. In particular, the planed EIC machine will be able to study the quark-antiquark jet correlation in DIS process, whereas RHIC and future LHC experiments shall provide information on direct photon-quark jet correlation in pA collisions.

The extension to the dijet-correlation in pA collisions is straightforward. The relevant initial and final state interaction phases have been calculated in Ref. [2]. To obtain the differential cross section in the correlation limit, we have to take the large N_c limit and the mean field approximation [7, 24]. After a lengthy calculation, we find

$$\frac{d\sigma^{(pA \to \text{Dijet}+X)}}{d\mathcal{P}.\mathcal{S}.}$$
$$= \sum_q x_1 q(x_1) \frac{\alpha_s^2}{\hat{s}^2}\left[\mathcal{F}_{qg}^{(1)} H_{qg \to qg}^{(1)} + \mathcal{F}_{qg}^{(2)} H_{qg \to qg}^{(2)}\right]$$
$$+ x_1 g(x_1) \frac{\alpha_s^2}{\hat{s}^2}\left[\mathcal{F}_{gg}^{(1)}\left(H_{gg \to q\bar{q}}^{(1)} + \frac{1}{2} H_{gg \to gg}^{(1)}\right)\right.$$
$$\left. + \mathcal{F}_{gg}^{(2)}\left(H_{gg \to q\bar{q}}^{(2)} + \frac{1}{2} H_{gg \to gg}^{(2)}\right) + \frac{1}{2}\mathcal{F}_{gg}^{(3)} H_{gg \to gg}^{(3)}\right] \; , \tag{14}$$

6

where again $q(x_1)$ and $g(x_1)$ are integrated quark and gluon distributions from the projectile nucleon. The hard partonic cross sections are defined as

$$H^{(1)}_{qg \to qg} = \frac{\hat{u}^2 \left(\hat{s}^2 + \hat{u}^2\right)}{-2\hat{s}\hat{u}\hat{t}^2}, \quad H^{(2)}_{qg \to qg} = \frac{\hat{s}^2 \left(\hat{s}^2 + \hat{u}^2\right)}{-2\hat{s}\hat{u}\hat{t}^2}$$

$$H^{(1)}_{gg \to q\bar{q}} = \frac{1}{4N_c} \frac{2\left(\hat{t}^2 + \hat{u}^2\right)^2}{\hat{s}^2\hat{u}\hat{t}}, \quad H^{(2)}_{gg \to q\bar{q}} = \frac{1}{4N_c} \frac{4\left(\hat{t}^2 + \hat{u}^2\right)}{\hat{s}^2}$$

$$H^{(1)}_{gg \to gg} = \frac{2\left(\hat{t}^2 + \hat{u}^2\right)\left(\hat{s}^2 - \hat{t}\hat{u}\right)^2}{\hat{u}^2\hat{t}^2\hat{s}^2}, \quad H^{(2)}_{gg \to gg} = \frac{4\left(\hat{s}^2 - \hat{t}\hat{u}\right)^2}{\hat{u}\hat{t}\hat{s}^2}$$

$$H^{(3)}_{gg \to gg} = \frac{2\left(\hat{s}^2 - \hat{t}\hat{u}\right)^2}{\hat{u}^2\hat{t}^2}, \tag{15}$$

and the various gluon distributions of nucleus A are defined as

$$\mathcal{F}^{(1)}_{qg} = xG^{(2)}(x, q_\perp), \quad \mathcal{F}^{(2)}_{qg} = \int xG^{(1)}(q_1) \otimes F(q_2),$$

$$\mathcal{F}^{(1)}_{gg} = \int xG^{(2)}(q_1) \otimes F(q_2), \quad \mathcal{F}^{(2)}_{gg} = -\int \frac{q_{1\perp} \cdot q_{2\perp}}{q_{1\perp}^2} xG^{(2)}(q_1) \otimes F(q_2),$$

$$\mathcal{F}^{(3)}_{gg} = \int xG^{(1)}(q_1) \otimes F(q_2) \otimes F(q_3), \tag{16}$$

where $\otimes$ represents the convolution in momentum space: $\int \otimes = \int d^2q_1 d^2q_2 \delta^{(2)}(q_\perp - q_1 - q_2)$. Clearly, this process depends on both UGDs in a complicated way, and the naive k_t-factorization does not hold. We have checked the above results in different kinematics. First, we recover the inclusive dijet cross section by integrating over $q_\perp$. Second, in the dilute limit of A, or equivalently at large $q_\perp$: $P_\perp \gg q_\perp \gg Q_S, \Lambda_{QCD}$, we reproduce the dijet-correlation in the collinear factorization approach [3]. Last but not least, we find the CGC calculation agrees with above results perfectly.

Recently, both STAR and PHENIX Collaborations have published experimental results on di-hadron correlations in dAu collisions, where a strong back-to-back de-correlation of the two hadrons was found in the forward rapidity region of the deuteron [25]. These results have been compared to a number of theoretical calculations in the CGC formalism, where different assumptions have been made in the formulations [26–28]. In particular, the numerical evaluation in Ref. [26] only contains the first term in the qg channel in Eq.(14). The missing term is equally important and should be taken into account to interpret the STAR data. We plan to compare our results to these calculations and those in Ref. [29] for $q\bar{q}$ production in pA collisions in a future publication[24], together with detailed derivations of generalized results illustrated in this paper.

In summary, we have studied the k_t-factorization for dijet production at small-x in nuclei. We found that different gluon distributions probed in different dijet production processes can be built from two basic building blocks, the Weizsäcker-Williams distribution and the Fourier transform of the dipole cross section. The most important result is that the DIS dijet process can directly measure the well-known WW gluon distribution which would be very interesting physics to pursue at the planned EIC.

[1] D. Boer and W. Vogelsang, Phys. Rev. D **69**, 094025 (2004).

[2] C. J. Bomhof, P. J. Mulders and F. Pijlman, Eur. Phys. J. C **47**, 147 (2006).

[3] J. W. Qiu, W. Vogelsang and F. Yuan, Phys. Lett. B **650**, 373 (2007); Phys. Rev. D **76**, 074029 (2007).

[4] J. Collins and J. W. Qiu, Phys. Rev. D **75**, 114014 (2007).

[5] W. Vogelsang and F. Yuan, Phys. Rev. D **76**, 094013 (2007); J. Collins, arXiv:0708.4410 [hep-ph].

[6] T. C. Rogers and P. J. Mulders, Phys. Rev. D **81**, 094006 (2010).

[7] B. W. Xiao and F. Yuan, Phys. Rev. Lett. **105**, 062001 (2010); arXiv:1008.4432 [hep-ph].

[8] L. V. Gribov, E. M. Levin and M. G. Ryskin, Phys. Rept. **100**, 1 (1983).

[9] A. H. Mueller and J. w. Qiu, Nucl. Phys. B **268**, 427 (1986).

[10] L. D. McLerran and R. Venugopalan, Phys. Rev. D **49**, 2233 (1994); Phys. Rev. D **49**, 3352 (1994).

[11] E. Iancu, A. Leonidov and L. McLerran, arXiv:hep-ph/0202270; E. Iancu and R. Venugopalan, arXiv:hep-ph/0303204; J. Jalilian-Marian and Y. V. Kovchegov, Prog. Part. Nucl. Phys. **56**, 104 (2006); F. Gelis, E. Iancu, J. Jalilian-Marian and R. Venugopalan, arXiv:1002.0333 [hep-ph]; and references therein.

[12] A. Deshpande, R. Milner, R. Venugopalan and W. Vogelsang, Ann. Rev. Nucl. Part. Sci. **55**, 165 (2005).

[13] see e.g., D. Kharzeev, Y. V. Kovchegov and K. Tuchin, Phys. Rev. D **68**, 094013 (2003).

[14] J. C. Collins and D. E. Soper, Nucl. Phys. B **194**, 445 (1982).

[15] X. d. Ji, J. P. Ma and F. Yuan, JHEP **0507**, 020 (2005).

[16] A. V. Belitsky, X. Ji and F. Yuan, Nucl. Phys. B **656**, 165 (2003).

[17] Y. V. Kovchegov and A. H. Mueller, Nucl. Phys. B **529**, 451 (1998).

[18] S. J. Brodsky, P. Hoyer, N. Marchal, S. Peigne and F. Sannino, Phys. Rev. D **65**, 114025 (2002).

[19] J. C. Collins and T. C. Rogers, Phys. Rev. D **78**, 054012 (2008).

[20] F. Gelis and A. Peshier, Nucl. Phys. A **697**, 879 (2002).

[21] F. Dominguez, C. Marquet and B. Wu, Nucl. Phys. A **823**, 99 (2009).

[22] R. Baier, A. Kovner, M. Nardi and U. A. Wiedemann, Phys. Rev. D **72**, 094013 (2005).

[23] F. Gelis and J. Jalilian-Marian, Phys. Rev. D **66**, 014021 (2002).

[24] F. Dominguez, C. Marquet, B.W. Xiao, F. Yuan, to be published.

[25] E. Braidot, for the STAR Collaboration, arXiv:1008.3989 [nucl-ex]; B. Meredith, for the PHENIX Collaboration, to appear;

[26] C. Marquet, Nucl. Phys. A **796**, 41 (2007); J. L. Albacete and C. Marquet, Phys. Rev. Lett. **105**, 162301 (2010).

[27] J. Jalilian-Marian and Y. V. Kovchegov, Phys. Rev. D **70**, 114017 (2004).

[28] K. Tuchin, Nucl. Phys. A **846**, 83 (2010).

[29] J. P. Blaizot, F. Gelis and R. Venugopalan, Nucl. Phys. A **743**, 57 (2004).